Enhancing chloride ion penetration resistance into concrete by using graphene oxide reinforced waterborne epoxy coating

W. Zheng[1], W.G. Chen[1*], T. Feng,[1] W.Q.Li,[1] X.T. Liu [2], L.L. Dong[3], Y.Q. Fu[2, *]

[1] School of Materials Science and Engineering, Xi'an University of Technology, Xi'an, Shaanxi, 710048, P.R. China

[2] Faculty of Engineering and Environment, Northumbria University, Newcastle upon Tyne, NE1 8ST, UK.

[3] Advanced Materials Research Central, Northwest Institute for Nonferrous Metal Research, Xi'an, Shaanxi, 710071, P.R. China

Abstract: To prevent early failure of concrete due to infiltration of chloride ions from environment, epoxy resin nanocomposites modified with graphene oxides (GOs) were prepared using a solution blending process and then sprayed onto testing blocks of concrete. Microstructural analysis revealed that the GOs were uniformly dispersed inside the epoxy matrix, and covalent cross-links were formed between the GO and epoxy matrix. Water surface contact angles of concrete coated with the nanocomposites coatings were found to increase firstly but then decrease with the increase of the added GO contents. When the GO content was 0.3 wt%, the contact angle was 96.1°±0.3°, whereas that of pure epoxy resin was 77.5° ±0.3°. At the same

[1] Corresponding authors: Professor Wenge Chen;Prof.Richard Y.Q.Fu.
E-mail: wgchen001@263.net (W.G. Chen), richard.fu@northumbria.ac.uk (Richard Y.Q. Fu)

GO content, water absorption and chloride diffusion coefficient of the coated concrete are much lower than those of the uncoated samples. The enhancement mechanisms for the chloride ion penetration resistance are attributed to the formation of cross-linking in the composite coating, improved hydrophobicity and shielding effects of the GOs.

Key words: graphene oxide, waterborne epoxy coating, interfacial structure, concrete, chloride ion permeability

1. Introduction

Concrete has wide-range applications for constructions, buildings, bridges and roads, and it has a better durability compared to metal. Generally, concrete is considered to be non-corrosive, but in fact the erosive medium in the environment will have physical or chemical influences to its structures after a short term service, thus resulting in their early failures [1–3]. Epoxy coating with epoxy resin as the main component can form a dense layer on the surface of concrete after curing [4], which can prevent the erosive medium to penetrate into the concrete and enhance its durability [5]. However, previous studies showed that the protective effect of the epoxy coating on the concrete is not always effective, as the erosive medium (such as solutions with OH^- and Cl^-) could slowly penetrate through the coating and react with the concrete [6].

The corrosion resistance of the coatings becomes an important parameter linking to their long-term durability, thus it is crucial to modify the epoxy coatings, for

example, using suitable nanofillers to enhance their corrosion resistance [7,8]. However, nanoparticles are easily agglomerated inside the organic matrix due to their large specific surface areas and high surface energy values. Meanwhile, existence of nanoparticles will often create defects inside the organic coating, which deteriorates the coating's performance [9]. For examples, Li et al. [10] reported the influence of nanoparticles on hydrophobicity of organic film coated concrete, and they showed that moderate incorporation of nanoparticles can increase contact angles of water on the concrete surface and reduce water absorption. Leung et al. [11] reported that addition of organoclay nanoparticles can effectively improve the protective effect of organic coatings on concrete, thus enhancing moisture resistance and improving the resistance of chloride ion penetration into the concrete.

Recently, graphene and its derivatives have been explored as nanofillers for the organic coatings due to their unique nanostructures, superior ion-diffusion barrier properties, large specific surface areas and good compatibility with polymer matrix [12,13,14]. For example, Yousefi et al. [15] prepared polyurethane composite coatings doped with reduced graphene oxide (rGO), and proved that the rGO can be used as a moisture barrier in the polyurethane coatings. Zhang et al. [16] studied the effect of polyvinylpyrrolidone/reduced graphene oxide (PVP/rGO) on the corrosion resistance of epoxy coatings and revealed that the incorporation of PVP/rGO nanosheets significantly improved the erosion resistance of this coating.

Compared with graphene, graphene oxide (GO) can be easily and uniformly dispersed in water due to their carboxylic acid groups at their edges and epoxy and

hydroxyl groups on the basal planes [17]. Therefore, during a solution blending process, GO can achieve a better dispersion in waterborne polymer matrix. Li et al. [18] prepared series of graphene oxide modified waterborne polyurethane-acrylate hybrids and proved that graphene oxide in the hybrid has a good dispersion. Javidparvar et al. [19] reported that an epoxy-polyamide composite coating with GO could be used for storage and targeted releases of cerium cation inhibitors on the steel corrosion sites. Although there are many studies on corrosion protection of metals using graphene-based organic coatings, as far as we know, there are few studies on enhancing the durability of concrete coated with the graphene-based organic coatings.

In this work, waterborne epoxy nanocomposite coatings were prepared using a solution blending process with the graphene oxide (GO) as the reinforcement agency. The nanocomposite coating was sprayed onto the surface of concrete testing blocks. Microstructures of the nanocomposite coatings were characterized, and surface contact angles and impermeability of the coated concrete were tested. Finally, the enhancement mechanisms of the composite coatings were discussed.

2. Experimental

2.1. Raw materials

Raw materials of the concrete were composed of ordinary Portland cement (produced by Yaobai Co., Ltd, Shaanxi, China), natural river sand, gravel (diameters from 5 to 25 mm), tap water and water reducer (HS-109, Yizheng Heshengbang Building Material Co., Ltd., China), following the Chinese National Standard

(JGJ55-2011). The mixed ratio of different components of concrete are listed in Table 1. The waterborne epoxy resin (bisphenol A type, E-51) and aliphatic amine curing agent (F705) were obtained from Shenzhen Jitian Chemical Co., Ltd., which follows the standard requirements of Chinese specification of film-forming coatings for concrete structure protection (JG/T 335-2011). Natural flakes of graphite (200 mesh, purity 99.9 %) and the other reagents (including H_2SO_4, $KMnO_4$, $NaNO_3$ and HCl) were obtained from Sinopharm Chemical Reagent Co. Ltd. Shanghai, China. All the chemicals were used directly without further purification.

2.2. Preparation of GO dispersion

The conventional Hummer's method was employed to synthesize graphene oxide [20]. Typical experimental procedures are listed as follows: (a) 5 g of graphite powder was mixed with 2.5 g of $NaNO_3$ and 150 mL of concentrated H_2SO_4, and the mixture was stirred at an ice-bath environment for 30 min; (b) 30 g of $KMnO_4$ was added slowly into the mixture and held for 120 min with a constant agitation in an ice bath (≤5℃). (c) The temperature was then increased to 35℃ in a water bath and the solution was kept for 3 hrs. (d) The temperature was then increased to 90 ℃, and 200 mL of purified water was added gradually into the system and stirred for 30 min. The mixture of suspension was washed with 10% HCl (to remove SO_4^{2}) and deionized water for many times (≥20 times). The products were dried using a vacuum freeze-drying method and the dried products were kept at 40℃ for 48 hrs. Finally the obtained GO powders and deionized water were mixed with a ratio of 2~4 mg to 1 ml and ultrasonically dispersed for 60~90 minutes in order to obtain a GO dispersed

solution.

2.3. Fabrication of coated concrete specimens

Based on the mass percentages of epoxy monomer and curing agent added into the composites, 0wt.%, 0.1wt.%, 0.3wt.%, 0.5wt.% of GOs were added into the epoxy coating. The total mass of epoxy monomer and curing agent was 7 g. The epoxy monomer of 5 g was diluted with an excessive amount of deionized water for easy stirring. By keeping a total volume of 25 ml of the mixture, GO solution with an appropriate concentration (in the range of 2 ~ 4 mg/ml depending on the amount of GO added) was mixed with the prepared epoxy resin solvent, and the mixture was ultrasonically dispersed for 30 min. The water-based curing agent of 2 g and antifoaming agent of 4 ml were added inside the prepared epoxy to obtain the nanocomposite paints. The nanocomposite paints were slowly stirred for 3 min, and then transferred into a vacuum chamber for half an hour to remove any bubbles inside. The concrete specimens with a shape of 100 mm (length)×100mm (width) ×50mm (height) were fabricated and cured for 28 days in a standard curing room. One surface (100mm×100mm) of these concrete specimens was polished with sandpapers, cleaned, and dried inside an oven at 60℃ for 48 hrs in air. The prepared nanocomposite paints were sprayed uniformly onto the polsihed surface of the concrete specimens using a spray gun. The spray process parameters are listed in Table 2. After spraying, the specimens were placed in an oven at 50°C and cured for 12 hours.

2.4. Characterization

Fourier-transform infrared spectroscopy (FTIR) was used to characterize the

epoxy coatings with and without additions of GOs, and a TENSOR 27 FT-IR spectrometer was used to identify the changes of functional groups of the epoxy resin and the chemical bonds between the graphene and epoxy matrix. The tested sample was ground into powders and mixed with KBr powders, then pressed into a disk with a diameter of 10 mm at 80 MPa before testing. The scan range of the wave number was 4000 cm^{-1} to 400 cm^{-1} with a resolution of 4 cm^{-1}. The chemical states of the GOs were characterized using an AXIS ULTRA X-ray photoelectron spectroscopy (XPS) within the energy range of 0-1200 eV. The XPS spectra were fitted using an XPS peak 4.1 software in which a Shirley background was applied. Surface morphology of the coating was observed using a scanning electron microscope (SEM, TM4000-PLUS). The nanocomposite coating samples with 0 wt.%~0.5 wt.% GO were cut into a 50 nm thick slice using a cryo-ultramicrotome machine, and microstructures and distributions of graphene inside the epoxy resin were characterized using a high resolution transmission electron microscope (HR-TEM, FEI-Talos F200X).

Surface contact angles of water droplets on coated and uncoated concrete specimens were measured using an OCA20 contact angle measurement instrument. Water absorption of concrete was characterized based on the following procedures. All uncoated sides of the coated concrete specimens were sealed using paraffin, and the same side of a uncoated concrete specimen was also sealed using the paraffin. Then these concrete specimens were immersed in water for 48 hours. After this process, the surface water of the concrete specimens was removed and their mass changes were measured. The water absorption ratio was calculated using the Eq.(1):

$$P = \frac{W - W_0}{W_0} \times 100\% \quad (1)$$

where P is the water absorption ratio of concrete specimen (%), W is the weight of the concrete specimen after soaking (g), W_0 is the weight of the concrete specimen before soaking (g).

The hardness of the nanocomposite coatings with different GO contents were tested using a Shore A sclerometer. The indenter of the sclerometer was pressed onto the surface of the coating until the bottom surface of the sclerometer is in a full contact with the coating. The scale on the hardness tester will indicate the hardness value of the coating. The same sample was tested at five different positions of the sample, and the average hardness results were obtained.

Chloride resistance of the coated concrete specimens was tested using a chloride ion permeation method. The concrete specimens with and without coating were sealed using the paraffin for all the uncoated areas. The filter paper soaked with a 5% NaCl solution was applied on the surface of the unsealed side of the concrete specimen. The concrete specimen was repeatedly wetted with the 5% NaCl solution using the filter paper for every 4 hours for 72 hrs in total. The specimens were cleaned and dried in an oven at 60 °C for 24 hrs, and then cut perpendicularly to the coating surface. The ground powders were collected from the different sections of the sample, e.g., from top to bottom of the sample with an interval distance of 5 mm. The collected powder was then filtered through a 0.63 mm sieve. Approximately 2 g of powder was collected from each position, added into 50 ml of deionized water, and ultrasonically dispersed for 30 min. After waiting for 2 hrs, the concentration of free chloride ions in

the liquid was measured according to the Chinese National Standard (JGJ/T322-2013), and then the concentration of water-soluble chloride ions in the concrete specimen was obtained using the Eq.(2):

$$C_{cl^-} = \frac{\frac{C_{AgNO_3} V_1}{V_2} \cdot V_3 \cdot M_{cl^-}}{m_p} \times 100\% \quad (2)$$

where C_{cl}^- is the percentage of free chloride ions in the powder (%), C_{AgNO3} is the millimolar concentration of the silver nitrate solution (mmol/mL), and V_1 is the silver nitrate solution volume (mL). V_2 is the volume of the liquid required for titration (mL), V_3 is the volume of deionized water (mL) dissolving the powder, and M_{cl}^- is the molar mass of chloride ion (g/mmol), m_p is the powder mass (g).

3. Results and discussion

3.1. Microstructure of graphene oxide

Generally, GO has various reactive oxygen functional groups such as epoxy and hydroxyl groups on the basal plane and carboxylic acid groups at the sheet edges. FT-IR spectroscopy was generally used to confirm the functional groups of the GO. The obtained FT-IR spectra of graphite and GO are shown in Fig. 1(a). It can be seen that the spectrum of the graphite has two absorption peaks at 3431 cm^{-1} and 1624 cm^{-1}, respectively. The former is corresponding to the vibration mode of hydroxyl (–OH), which is caused by the moisture absorption of graphite powder. The latter is the vibration mode of C=C double bond. Compared with those of the graphite, FT-IR spectra of the GO show many characteristic peaks: e.g., a hump at 3431 cm^{-1}

(corresponding to O–H stretching vibration modes of the C–OH groups and water), and many narrower bands: e.g., 1726 cm^{-1} (C=O stretching vibration modes of carbonyl and carboxyl groups, which are existed at the GO sheet edges), 1624 cm^{-1} (C=C stretching mode, which can be assigned to skeletal vibrations from non-oxidized graphitic region), 1402 cm^{-1} (C–O bending vibration mode of hydroxyl groups), 1217 cm^{-1} (C–O bending vibration mode of epoxy groups), and 1068 cm^{-1} (C–O bending vibration mode from hydroxyl groups and epoxy groups). Results clearly show that the GO surface contains three oxygen-containing functional groups: e.g., hydroxyl group, carboxyl group and epoxy group.

To further investigate the chemical binding between the functional groups and carbon atoms, C1s XPS spectra of the different samples were recorded as shown in Fig. 1(b). The C1s XPS spectrum of the GO clearly shows four types of carbon binding states: e.g., the sp^2-hybridized C–C (~284.6 eV), the epoxy and hydroxyl carbon (C–O) (~286.5 eV), the carboxylate carbon (C=O) (287.8 eV) and the carboxyl (–COOH) (~291.8 eV). Based on the area analysis of C and O XPS peaks, the ratio of C and O atoms for the GO prepared in this study is 2.05, indicating that graphite has been fully oxidized. Table 3 lists the obtained percentage of functional groups of the GO in this work. Combined with FT-IR analysis result, it can be confirmed that the main oxygen-containing group in the GO is the hydroxyl one.

Figure 1(c) shows a TEM image of the obtained GO, with its wrinkled structures in certain area along with large smooth area. Figure1(c) also shows the corresponding selected area electron diffraction (SEAD) pattern of the GO, which is a hexagonal

diffraction pattern, indicating that the GO has a disordered structure along its a-b axis direction [13,21]. This pattern is generated because the formation of functional groups destroys the sp^2 structure of graphite. Figure 1(d) shows an HR-TEM image of the GO. The lattice fringes at the boundary layer clearly reveal that the number of atomic layers is about 3~4. The average width of each layer spacing was calculated to be about 0.35 nm, which is near to that of the (002) plane of graphite. Graphene oxides with such a structure and a thickness within the nanocomposite coating were reported to effectively resist the penetration of erosive medium [18].

3.2. Microstructures of graphene oxide/epoxy nanocomposite coating

Figure 2 shows the FT-IR spectra of the epoxy coatings before and after the addition of GO. It can be found that the nanocomposite coating after adding the GO shows a new absorption peak at 1109 cm^{-1} compared with that of the pure epoxy coating. Based on literature [22-25], this peak corresponds to the C–O stretching vibration mode of the aliphatic ether, indicating that there are aliphatic ethers existed in the nanocomposite coating.

Based on the XPS test results listed in Table 3, there are a large amount of hydroxyl groups on the surfaces of GO layer. They react with the epoxy groups on the epoxy monomer under the catalytic enhancement of the polyamine in the curing agent [26,27], thus the aliphatic ether was formed, which can strongly bond the GO and epoxy matrix.

Figure 3 shows SEM images of the surfaces of nanocomposite coatings with different GO contents. The surfaces of the coatings with lower GO contents (see Figs.

3(a), 3(b) and 3(c)) are relatively uniform and dense, whereas those with higher GO contents such as 0.5 wt% (see Fig. 3(d)) are rough with many micropores. There are two possible reasons for this roughening phenomenon. Firstly, adding a larger amount of GOs will increase the viscosity of the coating, and it is difficult to form a continuous and uniform coating during curing. Secondly, agglomeration of GO in the epoxy coating will cause the loss of moisture on the coatings, which will result in the formation of micropores.

Figure 4 shows TEM images of the composite coating with 0.3 wt.% GO, in which some black lines can be observed in a light background (see Figs. 4(a), 4(b) and 4(c)). The black lines are the GO sheet, and these features are similar to those of graphene/polymer composite reported in literature [28,29]. It can be seen from Fig. 4(c) that the GO sheets are curved and interconnected among each other, indicating that the GO sheets are flexible and can be deformed/dispersed uniformly within the epoxy coating. Such well-dispersed GO sheets in the coatings are beneficial for preventing the corrosive media to penetrate into the substrate, and also prolonging the penetration paths of the corrosive medium into the coating, both of which will improve the impermeability of the coating.

Figures 4(d) and 4(e) are high magnification TEM images of the composite coating, in which some micropore defects can be observed (see the arrows in Fig. 4(d)). The sizes of these micropores are estimated to be 10 to 100 nm. Fig. 4(e) shows that there are some GO sheets (marked in squares) accumulated around the void defects of the coating. SAED results of this area shown in Fig. 4(f) indicate they are

polycrystalline graphene, which verifies that the GOs are easily gathered together at the defects of the coatings. The presence of these void defects would be harmful for the good impermeability of the coating. However, in the nanocomposite coating, the GO sheet surrounding these void defects can effectively prevent the penetration of corrosive medium through defect, thus maintaining a good corrosion resistance.

3.3. Properties of graphene oxide/epoxy nano-composite coating

The measured Shore hardness values of nanocomposite coatings are shown in Fig. 5. The hardness of the nanocomposite coating is increased continually as the GO content is increased. From the FT-IR results discussed in the above sections, the GO and the matrix are covalently cross-linked, thus forming a good interfacial bonding between the GO and matrix. As we know that the GO has excellent mechanical properties, therefore, adding GO can enhance mechanical properties of the polymer coating, which has been well-reported in literature [27,30].

Hydrophobicity is an important property of coatings for paint applications, and surface contact angle on concrete, θ, is an important parameter for evaluating its hydrophobicity or hydrophilicity. Generally, if $\theta < 90°$, the surface of the material is more hydrophilic, and water droplets can easily penetrate into the capillary; if $\theta > 90°$, the surface of material is more hydrophobic, and water droplets are difficult to diffuse into the capillary. Figure 6 displays the measured results of water contact angles for both the uncoated and coated concrete samples with different GO contents. From Figs.6(a) and 6(b), the water contact angle on the concrete is obviously increased after it is coated with the epoxy layer, but still less than 90°. From Figs.6(c) to 6(e), the

wetting angle of the composite coating is increased firstly and then decreased with further increase of GO content. Although the GO is intrinsically hydrophilic, it reacts with the epoxy coating, then forms the chemicals which can act as hydrophobic agents [28], and thus enhances the overall hydrophobicity of the composite coating. However, because of the agglomeration of GOs at a very high content in the nanocomposite coating, the hydrophilicity of the nanocomposite coating becomes much poorer as the GO is hydrophilic (see Fig. 6(e)).

The wettability of a solid surface is determined by its chemical composition and microscopic surface structures [31]. It is well known that wettability is primarily affected by the chemical composition of the material surface, which determines the intrinsic contact angle of the surface. Effect of surface microstructure on wettability can be illustrated using the Wenzel's model [32] and the Cassie's model [33]. Previous studies showed that the Wenzel's model is suitable for materials with intrinsic wettability between moderately hydrophilic and moderately hydrophobic, whereas the Cassie's model is more suitable for materials with intrinsic wettability in highly hydrophilic or highly hydrophobic surfaces [34]. Therefore, for the GO/epoxy nanocomposite coatings, the relationship between the contact angle and surface roughness is more in line with the Wenzel's model, rather than the Cassie's model. According to Wenzel's model, at liquid-solid interface, the actual surface area will be much larger than the nominal surfaces because of its large surface roughness. Assuming that a liquid fills the groove structure on the surface, the relationship

between the apparent contact angle θ^* of the rough surface and the intrinsic contact angle θ of the smooth surface can be determined using the Eq.3 [32]:

$$\cos\theta^* = r\cos\theta \quad (3)$$

where r is defined as the roughness factor, e.g., the ratio of the actual surface area to the geometric surface area, and normally $r \geq 1$. Therefore, the surface roughness makes a hydrophobic surface ($\cos\theta<0$) appears more hydrophobic ($\cos\theta^*<\cos\theta$), and also the hydrophilic surface ($\cos\theta>0$) appears more hydrophilic ($\cos\theta^*>\cos\theta$). From the SEM observation, the surface of the coating with 0.5 wt% GO shows the roughest surface feature, thus the corresponding contact angle is significantly reduced as the coating is more hydrophilic. The measurement results of the contact angles indicate that the addition of an appropriate amount of GO can change the surface properties of the nanocomposite coating from hydrophilic to hydrophobic within a certain loading ratio (~0.3 wt%).

Water absorption is one of the important characteristics for evaluating hydrophilicity of materials. Figure7 shows water absorption results for the GO-coated and uncoated specimens. It can be seen that the water absorption rates of all specimen are increased rapidly in the early stage but become flat in the later stage. The saturated water absorption for the untreated sample is 5.14%, and this value is significantly reduced after the sample surface is treated with epoxy coating, indicating that epoxy coating can effectively prevent concrete from absorbing water. The saturated water absorption of the coated specimen is increased firstly but then decreased with the increase of GO content contents, similar to the changes of contact angles.

In general, there are three mechanisms of water adsorption and penetration in the coating [35]: e.g., (1) microscopic molecular penetration: in which water molecules penetrate along the micro-gaps in the polymer chains; (2) early penetration: in which water molecules penetrate in the micropores formed during solvent drying process due to solvent evaporation; (3) macroscopic penetration: in which water molecules penetrate through visible defects in the coating due to chemical or mechanical damage. For the coatings without apparent defects, the mechanisms of moisture adsorption/penetration are mainly microscopic molecular penetration and early penetration as explained above. The GO sheets can shield water molecules, so the nanocomposite coatings have a good resistance to the microscopic penetration of water molecules. The early penetration effect of water depends on the wettability and the number of micropores in the coating. The nanocomposite coating with 0.3 wt% GO is hydrophobic, and its saturated water absorption is the lowest. Whereas the nanocomposite coating with 0.5 wt% GO content shows many surface micropores and poor hydrophobicity, so the saturated water absorption is the highest.

Resistance to chloride ion penetration is the most important performance parameters in evaluating the long-term performance of sprayed coatings for the concrete. In this study, the chloride ion concentration profile into the concrete was used to quantitatively evaluate the chloride ion penetration resistance of the concrete specimens. Figure 8(a) shows the chloride ion concentration for specimens with and without the GO nano-composite coatings. It can be seen from Fig. 8(a) that the chloride ion contents for all the samples are decreased with the increase of depth into

the sample. However, the chloride ion concentration of the coated specimen is significantly lower than of the uncoated one under the same measurement depth, indicating that the epoxy coating has a good resistance to chloride ion penetration.

Chloride ion erosion of the coated concrete is a very complex process, involving different phenomena such as diffusion, infiltration and physicochemical adsorption [36]. The faster the chloride ion penetrates into the coated concrete, the larger the diffusion coefficient will be. The diffusion coefficient of chloride ions in concrete can be determined using the Equations (4), (5) and (6) [37]:

$$D_i = \frac{d_i^{\,2}}{2t\left(\Phi^{-1}\left(m_i\right)\right)^2} \tag{4}$$

$$m_i = \frac{1}{2}\left[1 - \frac{C_i\left(x,t\right)}{C_s}\right] + 0.5 \tag{5}$$

$$D_{cl^-} = \frac{\sum_{i=1}^{n} D_i}{n} \tag{6}$$

where $C_{(x,t)}$ is the chloride ion concentration at the measurement point (%), C_s is the chloride ion concentration at a distance of 5 mm from the surface (%), and d_i is the distance from the measurement point to the concrete surface (m) , t is the diffusion time (s), D_i is the chloride diffusion coefficient of the measuring point, and D_{cl}^- is the statistical value of the chloride diffusion coefficient in the concrete. The results of chloride diffusion coefficients for the coated specimens calculated based on equations (2) to (4) are shown in Fig. 7(b). It can be seen from Fig. 8(b) that the chloride diffusion coefficient is decreased firstly but then increased with the increase of GO contents. The nanocomposite coating with 0.3 wt.% GO has the best resistance to

chloride ion penetration due to homogenous dispersion and chemical bonding of GOs in the epoxy coating. However, when the GO content exceeds this critical value, the agglomeration of GO will cause generation of more defects, and then chloride ions can penetrate into the coating with water easily penetrating along these defects, thus resulting in a decrease in the resistance to chloride ion penetration of the nanocomposite coating.

From the microstructure and property analysis of the nanocomposite coating, it can be found that adding a moderate amount of GO can effectively improve the impermeability of the epoxy coating. Figure 9 shows the schematic mechanism for the reinforcement of GO on the epoxy coating. Pure epoxy coatings have some defects due to solvent evaporation during curing. The epoxy resin is hydrophilic, and the corrosive medium could slowly penetrate into the coating along the defects, and further into the concrete matrix (Fig. 9(a)). After adding GO in the coating, the filling of the GO sheets around the defects in the coating forms an effective barrier and thus prevents the penetration of the erosive medium (Fig. 9(b)). As the GO content is increased, its barrier effect is increased, and the hydrophobicity of the composite is also improved. Therefore, the impermeability of the composite coating is significantly increased (Fig. 9(c)). However, as the GO content is further increased, the defects in the composite coating are increased, and the hydrophobicity of the composite coating is decreased, thus causing a negative effect on the impermeability of the coating (Fig. 9(d)).

4. Conclusions

In this paper, GO/epoxy resin nanocomposite coatings were prepared using a solution blending process, and then sprayed onto the surfaces of the concrete test block. The following conclusions are obtained from this study:

(1) The hydroxyl groups on the surface of the GO chemically react with the epoxy coating and form aliphatic ether, and there are covalent bonds formed between the GO and the epoxy coating matrix. The interaction between the GO and the matrix allows the GO to be uniformly dispersed inside the epoxy matrix.

(2) With the increase of GO contents, the Shore hardness of GO/epoxy composite coatings has been increased, and the hydrophobicity and impermeability have been improved firstly but then decreased afterwards. When the amount of GO content is 0.3 wt.%, the composite material has the best overall performance.

(3) The enhancing mechanisms for the GO on the coating is mainly caused by the filling the defects and formation of a diffusion barrier due to the coating, followed by improving hydrophobic properties of coating through reacting with epoxy resin; whereas agglomerating of the GO in the coating and reducing the hydrophobicity and impermeability of the coating at a higher loading contents.

Acknowledgement

The authors would like to acknowledge the financial supports from Shaanxi Coal Industry Group United Fund of China (No.2019JLM-2), Xi'an Science research project of China (No.2017080CG/RC043) and Electrical Materials and Infiltration

Key Laboratory of Shaanxi Province Projects (No.17JS080), Newton Mobility Grant (IE161019) through Royal Society and the National Natural Science Foundation of China. Science and Technology Project of Weiyang District of Xi'an City（201857）.

References

[1]A.M.Neville. Properties of Concrete. LAP Lambert Academic Publishing, 1996, 36(4):838–844.

[2]X.Y. Pan, Z.G. Shi, C.J. Shi, et al., A review on concrete surface treatment Part I:types and mechanisms, Constr. Build. Mater. 132 (2017) 578–590.

[3]X.Y. Pan, Z.G. Shi, C.J. Shi, et al., A review on surface treatment for concrete part 2: performance, Constr. Build. Mater. 133 (2017) 81–90.

[4]R.S.Bauer. Epoxy resin chemistry. American Chemical Society;1979.

[5]M. Ibrahim, A.S. Al-Gahtani, M. Maslehuddin, et al., Use of surface treatment materials to improve concrete durability, J. Mater. Civ. Eng. 11 (1999) 36–40.

[6]A,Merah,M.M.Khenfer,Y.Korichi.The effect of industrial coating type acrylic and epoxy resins on the durability of concrete subjected to accelerated carbonation.J.Adhes.Sci.Technol, 2015,29(22), 2446–2460.

[7]A. Hooda, M.S. Goyat, R. Gupta, et al., Synthesis of nano-textured polystyrene/ZnO coatings with excellent transparency and superhydrophobicity, Mater.Chem. Phys. 193 (2017) 447–452.

[8]J.P. Zhou, Z.Y. Tan, Z.L. Liu, et al., Preparation of transparent fluorocarbon/TiO_2-SiO_2 composite coating with improved self-cleaning

performance and antiaging property, Appl. Surf. Sci. 396 (2017) 161–168.

[9]M.K. Sahnesarayi, H. Sarpoolaky, S. Rastegari, Effect of heat treatment temperature on the performance of nano-TiO_2 coating in protecting 316L stainless steel against corrosion under UV illumination and dark conditions,Surf. Coat. Technol. 258 (2014) 861–870.

[10]G.Li,J.Yue,C.H.Guo,Y.S.Ji.Influences of modified nanoparticles on hydrophobicity of concrete with organic film coating.Constr. Build. Mater.169 (2018) 1–7.

[11]C.K.Y.Leung, H.G.Zhu, J.K.Kim, R.S.C.Woo. Use of polymer/organoclay nanocomposite surface treatment as water/ion barrier for concrete. J. Mater. Civ. Eng.20(7)(2008) 484–492.

[12]J.C. Meyer, A.K. Geim, M.I. Katsnelson, K.S. Novoselov, T.J. Booth, S. Roth, The structure of suspended graphene sheets, Nature 446 (7131) (2007) 60–63.

[13]Y. Zhu, S. Murali, W. Cai, X. Li, J.W. Suk, J. Potts, et al., Graphene and graphene oxide: synthesis, properties, and applications, Adv. Mater. 22 (46) (2010) 3906–39.

[14]S.G.Zhou, Y.M.Wu, W.J.Zhao, J.J.Yu, F.W.Jiang, L.Q.Ma.Comparative corrosion resistance of graphene sheets with different structures in waterborne epoxy coatings.Colloid Surf. A-Physicochem. Eng. Asp.556(5)(2018) 273–283.

[15]N.Yousefi,M.M.Gudarzi,Q.Zheng,X.Lin,J.K.KimHighly aligned, ultralarge-size reduced graphene oxide/polyurethane nanocomposites: mechanical properties and moisture permeability. Compos. Pt. A-Appl. Sci. Manuf.49(2013) 42–50.

[16]Z. Zhang, W. Zhang, D. Li, Y. Sun, Z. Wang, C. Hou, L. Chen, Y. Cao, Y. Liu,Mechanical and anticorrosive properties of graphene/epoxy resin composites coating prepared by in-situ method, Int. J. Mol. Sci. 16 (2015) 2239–22

[17]D.R.Dreyer, S.Park, C.W.Bielawski, R.S.Ruoff. The chemistry of graphene oxide, Chem. Soc. Rev.39(1)(2009) 228–240

[18]P.Li, H.Ren, F.Qiu, J.Xu, D.Yang.Preparation and properties of graphene oxide-modified waterborne polyurethane-acrylate hybrids.Polym.-Plast. Technol. Eng.53(13)(2014) 1408–1416

[19]A.A.Javidparvar, R.Naderi, B.Ramezanzadeh.Epoxy-polyamide nanocomposite coating with graphene oxide as cerium nanocontainer generating effective dual active/barrier corrosion protection. Compos. Pt. B-Eng.172(2019) 363–375

[20]L.L. Dong, W.G. Chen, N. Deng, C.H. Zheng, A novel fabrication of graphene by chemical reaction with a green reductant, Chem. Eng. J. 306 (2016) 754–762.

[21O.C.Compton, S.T. Nguyen.Graphene oxide, highly reduced graphene oxide, and graphene: versatile building blocks for carbon-based materials,Small.6(2010) 711–723.

[22]S. Stankovich, R.D. Piner, S.B.T. Nguyen, R.S. Ruoff, Synthesis and exfoliation of isocyanate-treated graphene oxide nanoplatelets, Carbon 44 (15) (2006) 3342–3347.

[23]S. Park, K.S. Lee, G. Bozoklu, W. Cai, S.T. Nguyen, R.S. Ruoff, Graphene oxide papers modified by divalent ions-enhancing mechanical properties via chemical cross-linking, ACS Nano 2 (3) (2008) 572–578.

[24]S.Park, D.A. Dikin, S.B.T. Nguyen, R.S. Ruoff, Graphene oxide sheets chemically cross-linked by polyallylamine, J. Phys. Chem. C 113 (36) (2009) 15801–15804.

[25]Q.Y. Xing, W.W. Pei, R.Q. Xu, J. Pei, Basic organic chemistry, Higher Education Press, Beijing, 2005, p. 180 (in Chinese).

[26]Smith MB,March J. March's advanced organic chemistry: reactions, mechanisms, and structure, 5th edition.Hoboken: John Wiely & Sons. 2007:236.

[27]W.Zheng,W.G.Chen,Q.Zhao,S.X.Ren,Y.Q,Fu.Interfacial structures and mechanisms for strengthening and enhanced conductivity of graphene/epoxy nanocomposites.Polymer. 163 (2019) 171–177.

[28]H. Kim, A.A. Abdala, C.W. Macosko, Graphene/polymer nanocomposites, Macromolecules. 43 (16) (2010) 6515–6530.

[29]H. Kim, Y. Miura, C.W. Macosko, Graphene/polyurethane nanocomposites for improved gas barrier and electrical conductivity, Chem. Mater. 22 (11) (2010)3441–3450.

[30]D.G. Papageorgiou, I.A. Kinloch, R.J. Young, Mechanical properties of graphene and graphene-based nanocomposites, Prog. Mater. Sci. 90 (2017) 75–127.

[31]A. Shafaamri, R. Kasi, V. Balakrishnan, et al., Amelioration of anticorrosion and hydrophobic properties of epoxy/PDMS composite coatings containing nano ZnO particles, Prog. Org. Coat. 92 (2016) 54–65.

[32]R.N.Wenzel.Surface roughness and contact angle. J. Phys. Chem.C ,53(9)(1949) 1466–1467.

[33]A. B. D. Cassie． Contact angles.Discuss. Farady .Soc,3(1948)11.

[34]L.J.Zheng,X.D.Wu,Z.lou,D.Wu.Preparation of superhydrophobic surface by surface microstructure.Chin. Sci. Bull.49(17)(2004)1691–1699.(in Chinese)

[35]H.Margareta,C.M.Hansen.Water permeation in coatings.Prog. Org. Coat. 13(1985) 171–194.

[36]H.S.Shi, Q.Wang.Study on the influencing factors of chloride ion migration in concrete. J.Build. Mater. 7(3)(2004)286–290.(in Chinese)

[37]Q.Wang, X.Zhang, R.R.Fu. Methods to evaluate diffusion coefficient of Chloride ions in concrete.J. Shandong Jianzhu.Univ. 21(4)(2006) 288–290.(in Chinese)

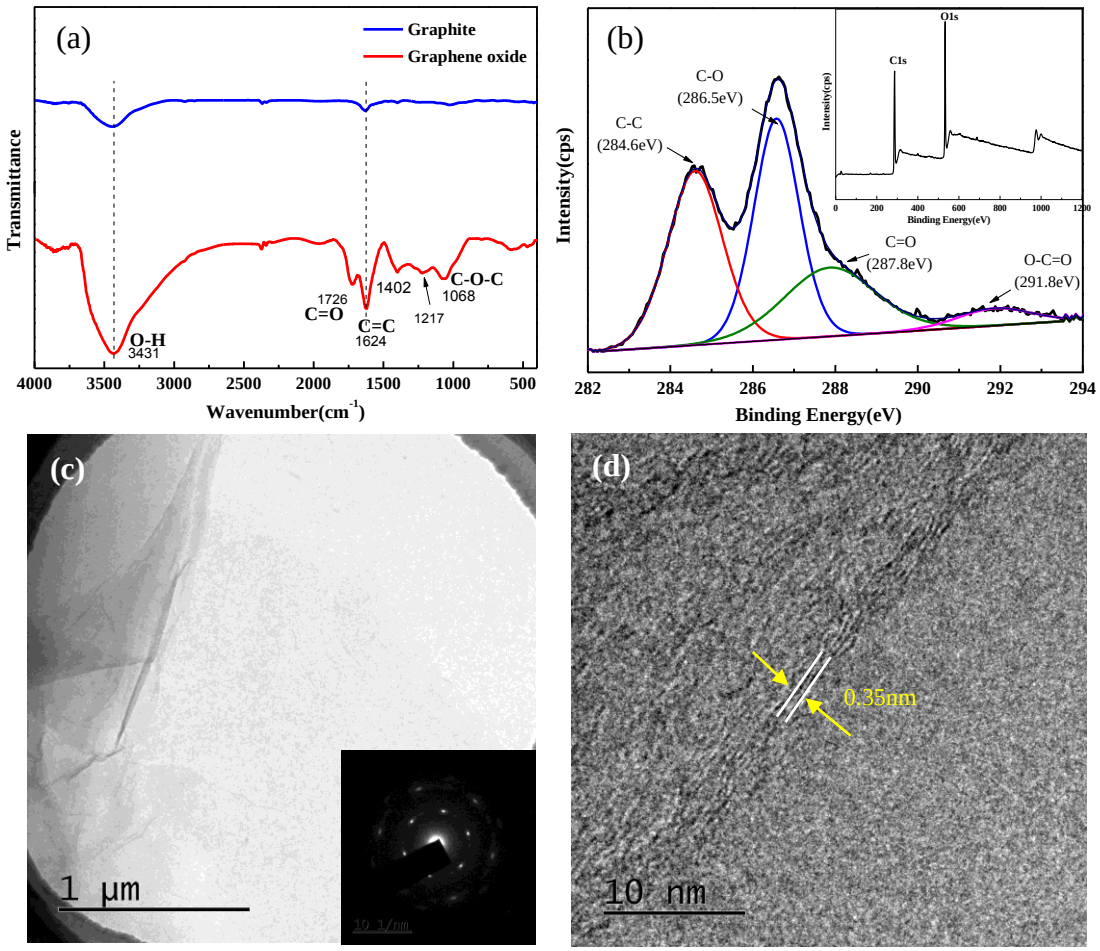

Fig. 1(a). FT-IR spectra of graphite and graphene oxide; (b) XPS spectra of C1s peaks for graphene oxide, The inset is XPS survey spectrum of GO; (c) TEM image and SAED pattern of

graphene oxide; (d) HR-TEM image of graphene oxide.

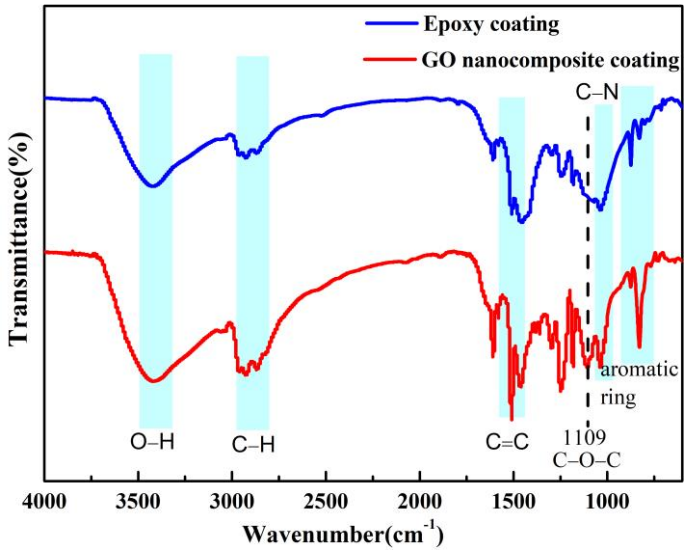

Fig.2 FT-IR spectra of the pure epoxy coating and 0.5 wt.% GO epoxy nanocomposite coating.

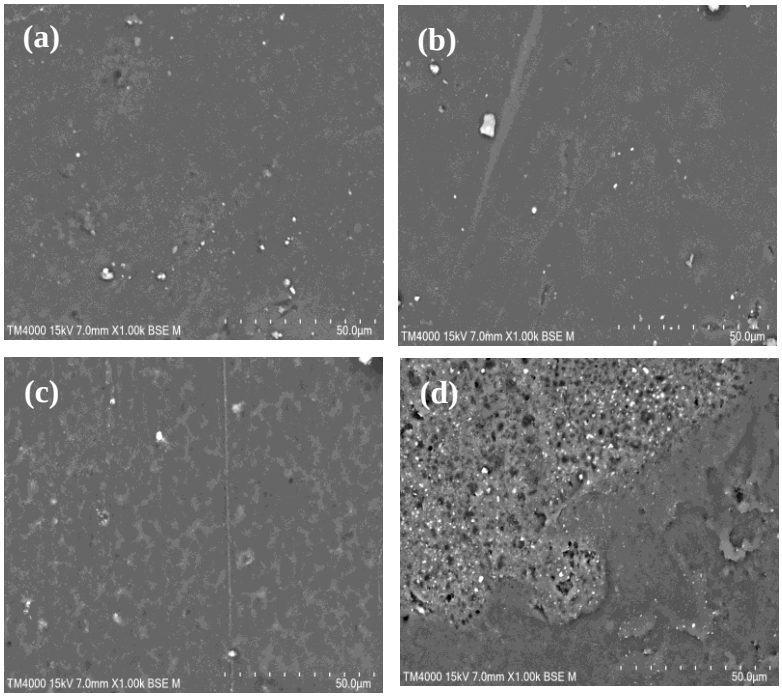

Fig.3.SEM images of surfaces of epoxy coating and nanocomposite coatings: (a) epoxy coating; and nanocomposites coatings of (b) 0.1 wt% GO ; (c) 0.3 wt% GO ; (d) 0.5 wt% GO .

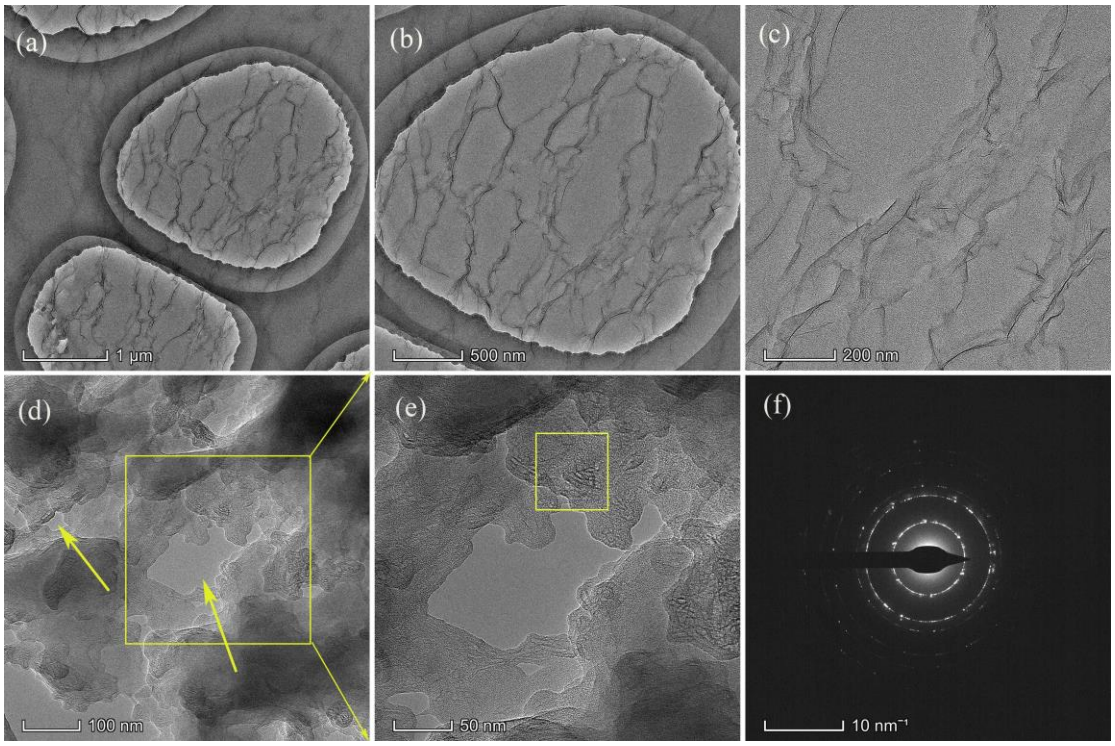

Fig.4.TEM images of nanocomposite coating with 0.3wt.% GO.(a) to (c):the low magnification images of defect-free areas of the coating,(d) and (e) :the high magnification images of the coating with defect, (f) : the SAED pattern of the box position in (e).

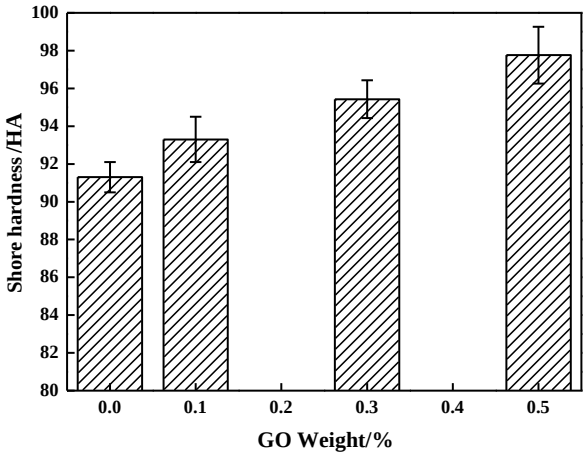

Fig.5.Shore hardness values of nanocomposite coatings with different GO contents.

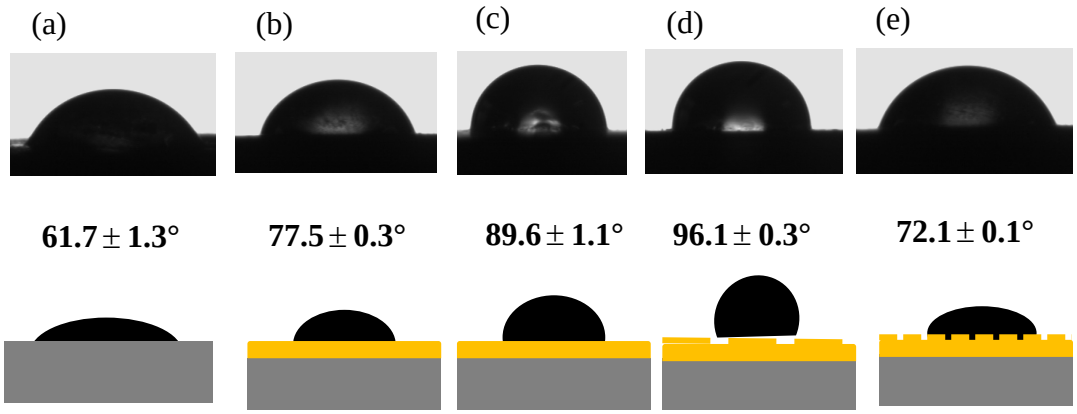

Fig.6. Water contact angle testing results of uncoated and coated concrete samples with different GO contents. (a) uncoated concrete; (b) with epoxy coating; nanocomposite coating with (c) 0.1 wt% GO; (d) 0.3 wt% GO; (e) 0.5 wt% GO.

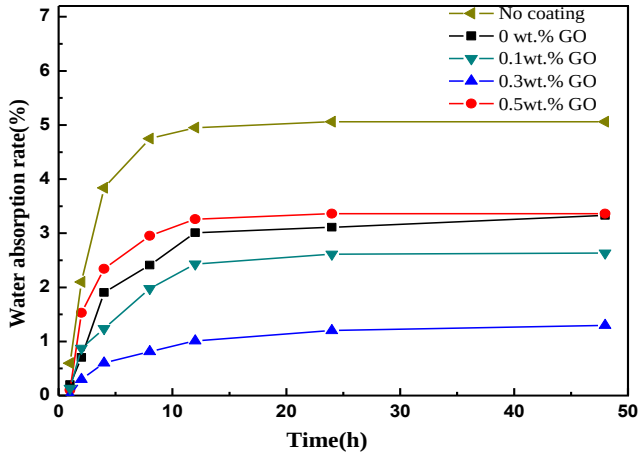

Fig.7. Water absorption of uncoated specimen and coated specimens with different GO contents.

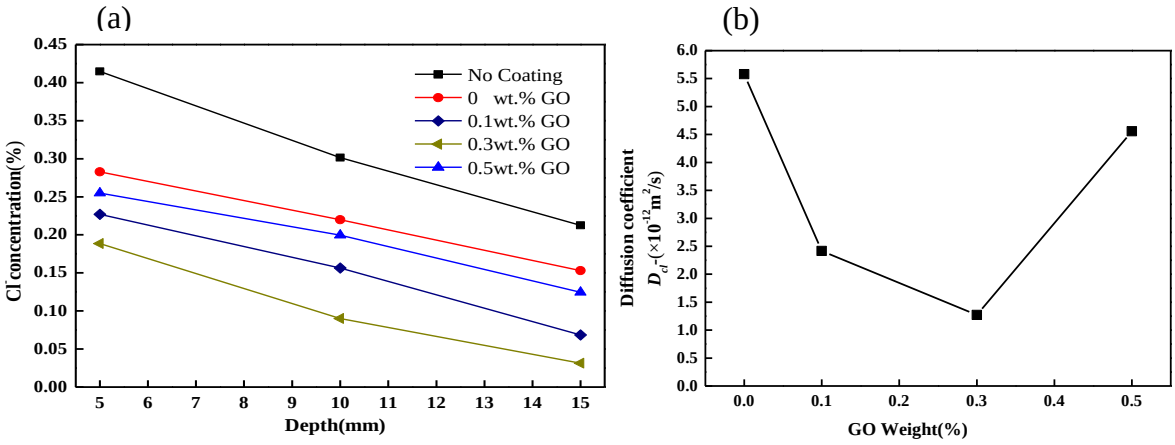

Fig.8 (a) Changes of chloride ion concentrations for uncoated and coated concrete specimens with different GO contents; (b) Chloride diffusion coefficient for uncoated and coated specimens with different GO contents.

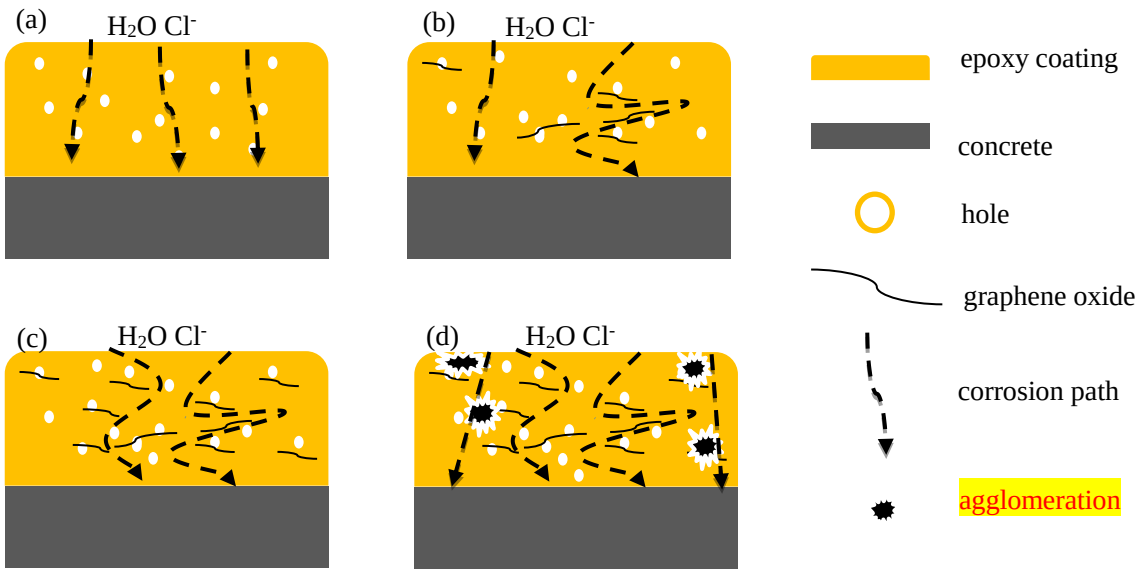

Fig.9. Reingorcement mechanisms of epoxy coating with different GO contents:(a) epoxy coating; nanocomposites of (b) 0.1 wt% GO ; (c) 0.3 wt% GO ; (d) 0.5 wt% GO.

Table.1 Mixture proportion of concrete(kg/m^3)

Item	Cement	Sand	Gravel	Water	Water reducer
Dosage	360	682	1150	234	2.5

Tabel.2 Spray process parameters for the coatings

Parameter	Value
Spraying time（s）	5s
Spray distance（mm）	150
gas pressure（MPa）	0.2-0.3
Spraying temperature（℃）	25
Spray gun moving rate（cm/s）	20-30
spray wide angle（°）	120
Spray gun caliber（mm）	200

Table.3 Binding energy and percentage of functional groups on the surface of graphene oxide

Binding energy(eV)	Chemical bond	Percentage (%)
284.8	–C–C–	42.8
286.4	–C–OH/–C-O-C-	39.7
287.8	–C=O	15.4
289.0	–COOH	2.1